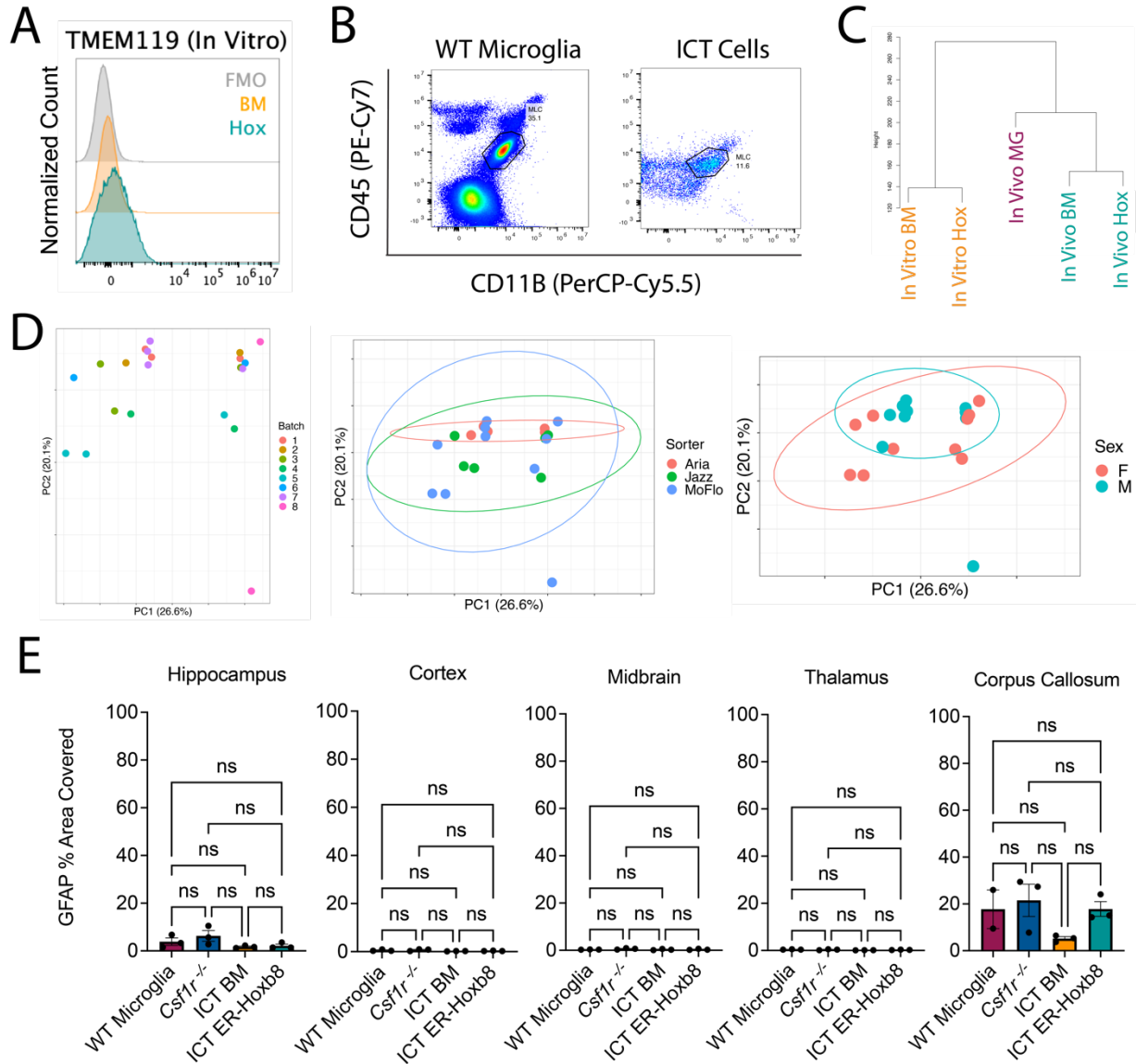
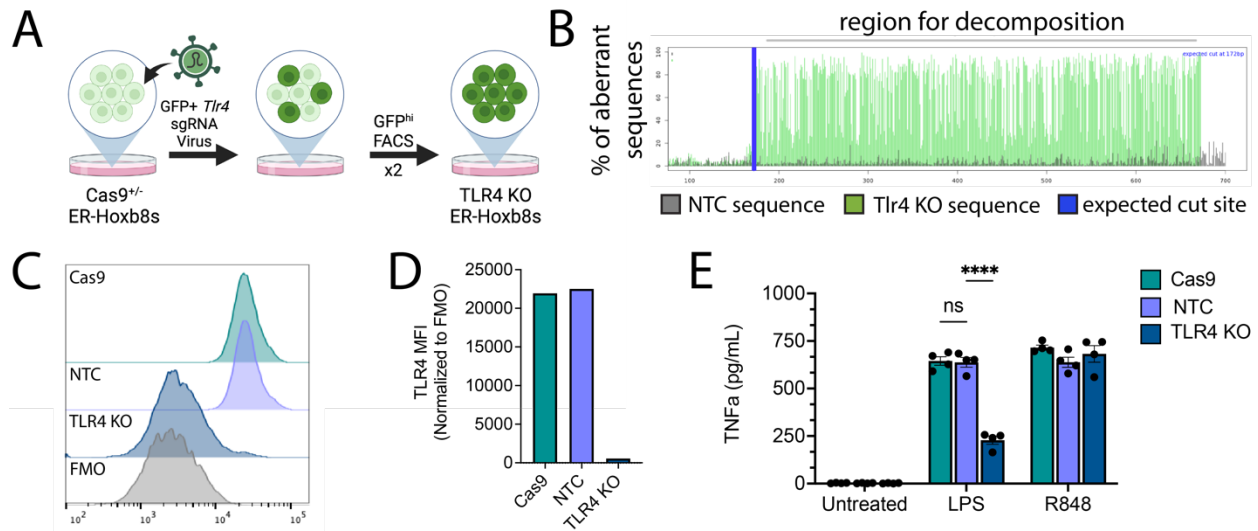


Supplemental Figure 1: Extended comparison of ER-Hoxb8 to BMD macrophages in vitro, relating to Figure 1. (A) Gating strategy for Figure 1C **(B)** Flow cytometry histograms and median fluorescence intensity (MFI) of CD11B (left) and CD45 (right), relating to Figure 1C **(C)** Heatmap showing Log2 CPM gene expression levels of macrophage genes across groups; progenitor and macrophage groups are as represented in Figure 1A, BM Mono = monocytes isolated from BM, 4div ER-Hoxb8 = ER-Hoxb8s collected after four days of in vitro differentiation **(D)** PCA plot combining bulk RNA sequencing data amongst all groups **(E)** Log2 CPM values of top 10 differentially expressed genes by Log2FC (CPM > 1, Log2FC >= 2, FDR < 0.05)

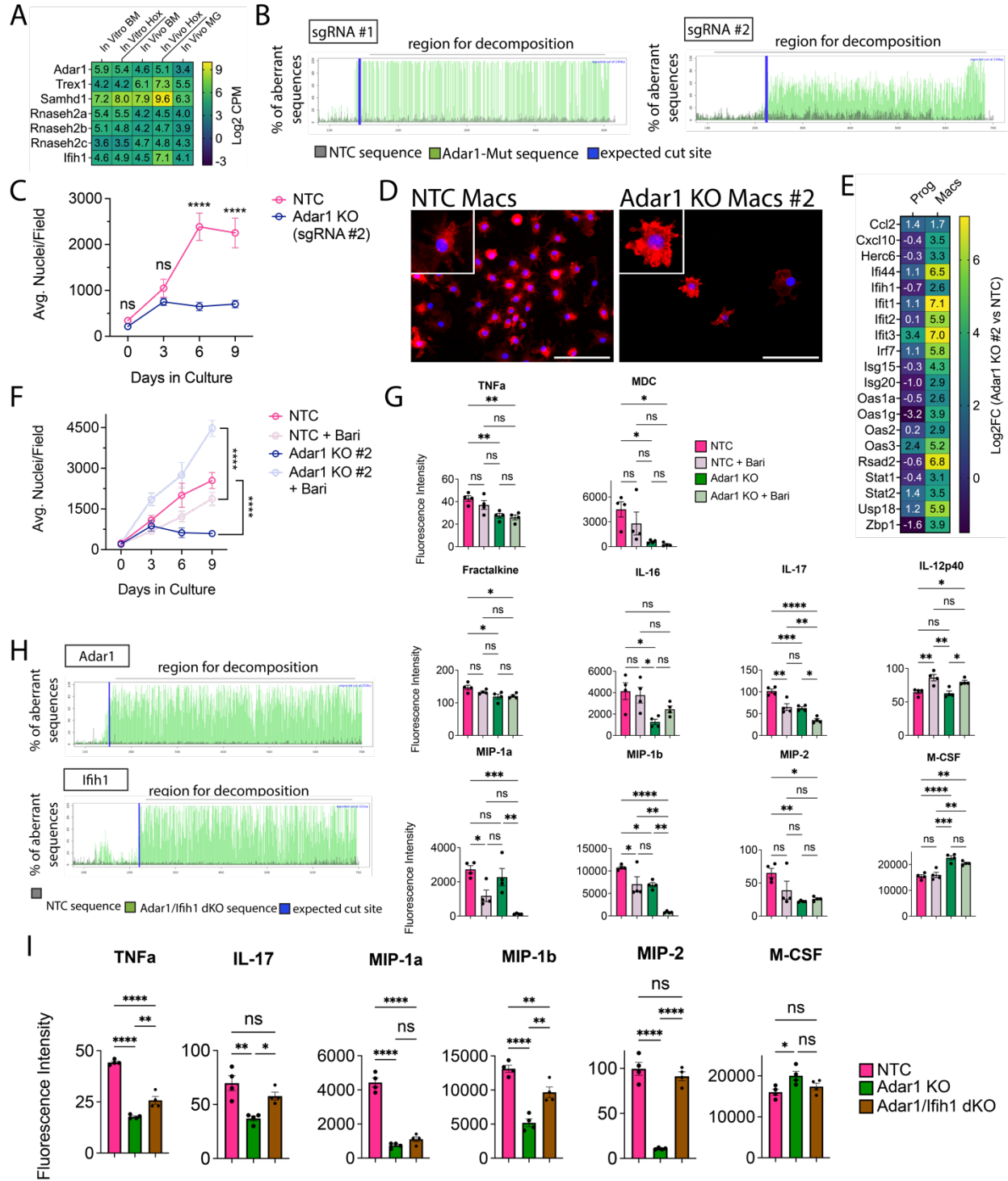


Supplemental Figure 2: Extended comparison of ER-Hoxb8 to BMD macrophages after intracranial transplantation in *Csf1r*^{-/-} hosts, relating to Figure 3. (A)

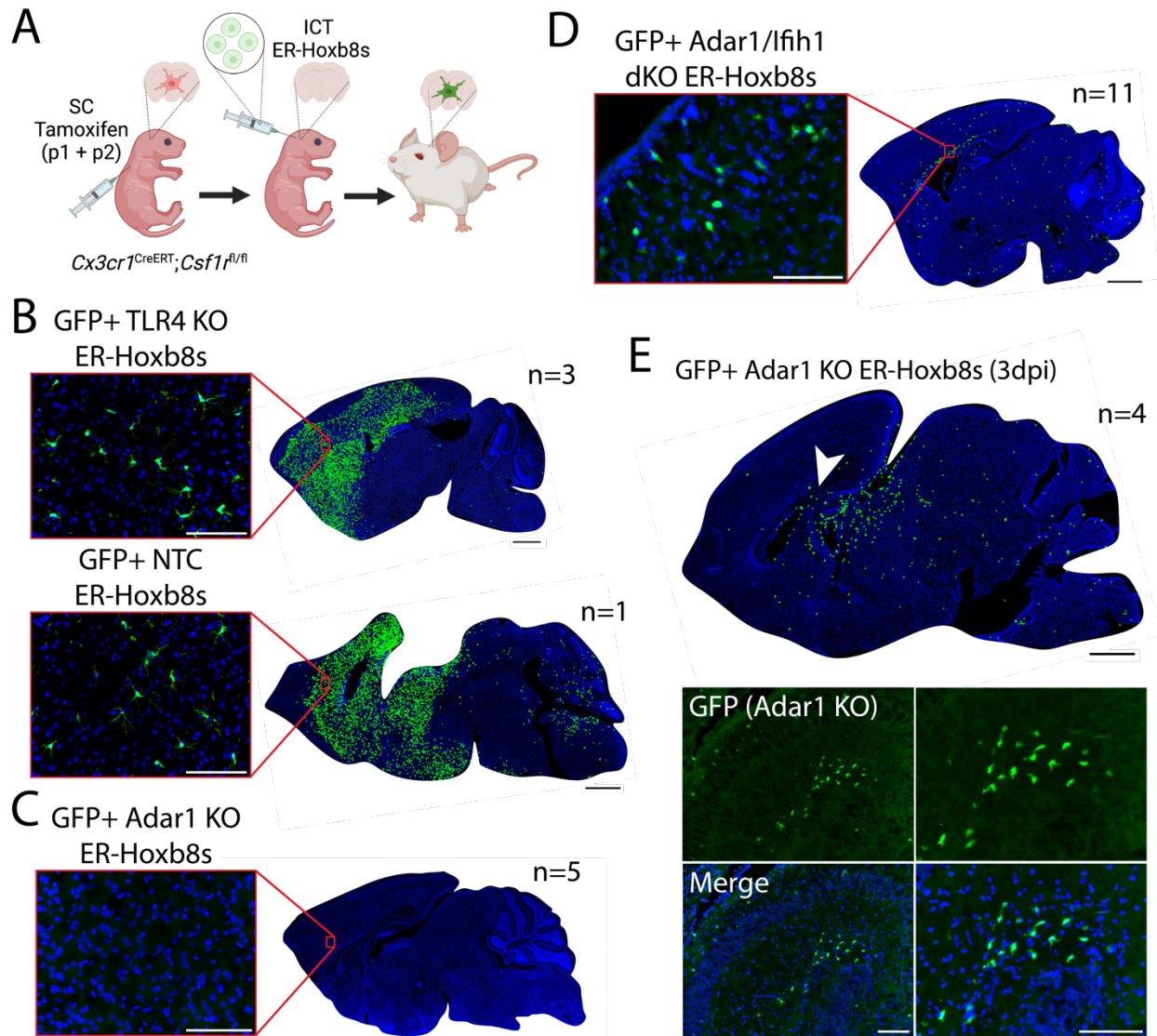
Histogram of TMEM19 surface staining by flow cytometry (pre-gated on live, singlet, leukocyte, CD45+/CD11b+) for seven-day differentiated in vitro BMD and ER-Hoxb8 macrophages (B) Gating strategy for in vivo TMEM19 histogram shown in Figure 3A (pre-gated on live, singlet, leukocyte, GFP) of WT microglia and intracranially transplanted (ICT) cells (BM or ER-Hoxb8s) (C) Unsupervised hierarchical cluster dendrogram, related to Figure 3B (distance method = euclidean; cluster method = complete) (D) Comparison of “batch” by PCA plots for harvest days (left), sorter used (middle), and host mouse sex (right) (E) Quantification of GFAP percent area covered; n = 3 biological replicates per group; each dot = one biological replicate (average area across three matched sagittal sections); p-values calculated via one-way ANOVA with multiple comparisons; ns = not significant or p >= 0.05, *p < 0.05, **p < 0.01, ***p < 0.001, ****p < 0.0001



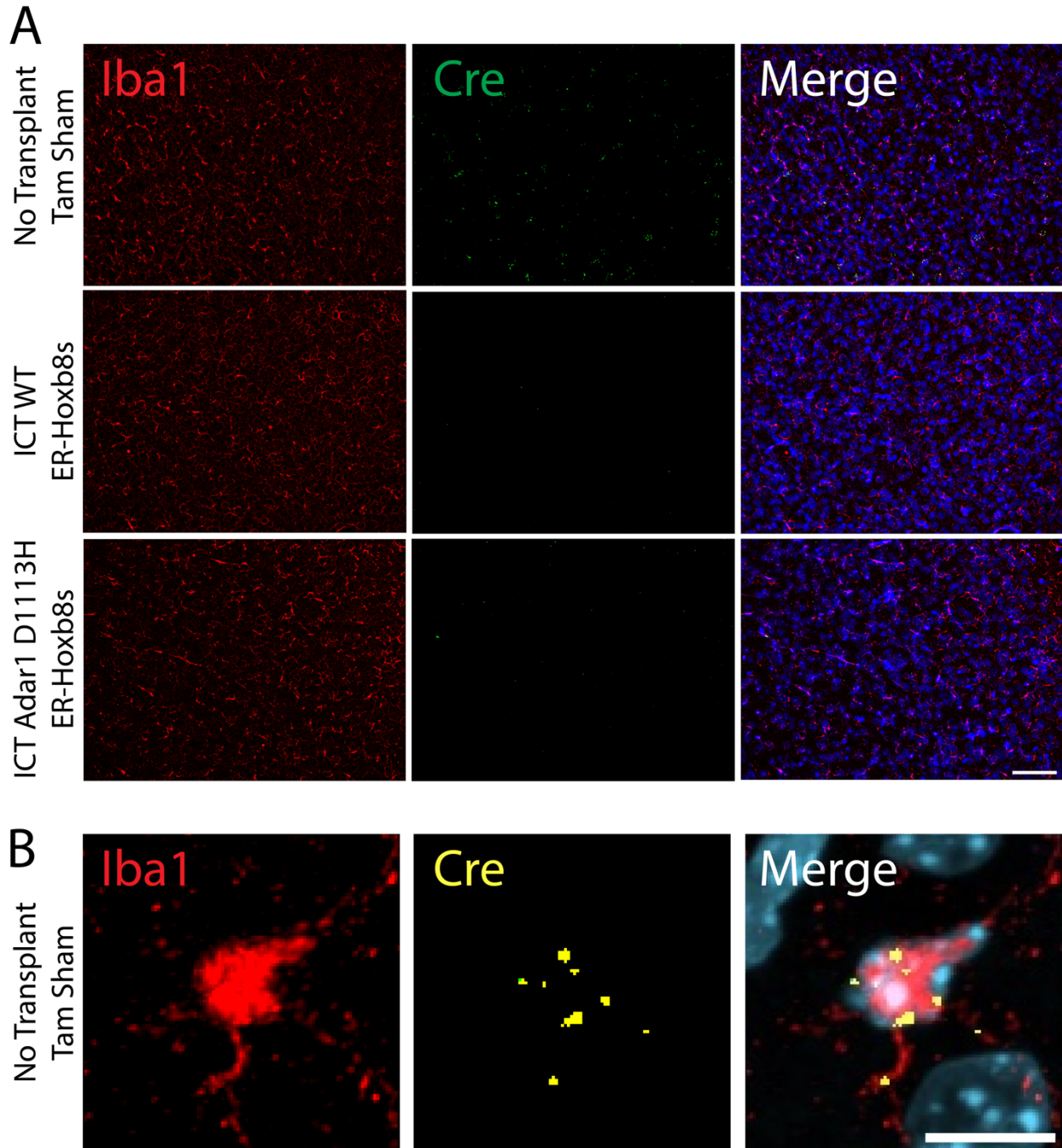
Supplemental Figure 3: CRISPR-Cas9 editing of ER-Hoxb8 progenitors, relating to Figures 4 and 5. (A) Schematic for *Tlr4* knockout using Cas9^{+/-} ER-Hoxb8s and sgRNA viral transduction (B) Post-editing trace decomposition charts (via TIDE Analysis) for *Tlr4* KO macrophages (C) Histogram of TLR4 surface staining by flow cytometry (pre-gated on live, singlet, leukocyte) for eight day-differentiated in vitro BMD and ER-Hoxb8 macrophages (D) TLR4 median fluorescence intensity (MFI) normalized to FMO levels using flow cytometry data shown in C (E) TNF α production, comparing control, LPS, and R848 treated samples (eight-day differentiation, 9.5h LPS or R848, 100ng/mL, n = four replicates per condition); p-values calculated via one-way ANOVA with multiple comparisons; ns = not significant or p \geq 0.05, *p < 0.05, **p < 0.01, ***p < 0.001, ****p < 0.0001



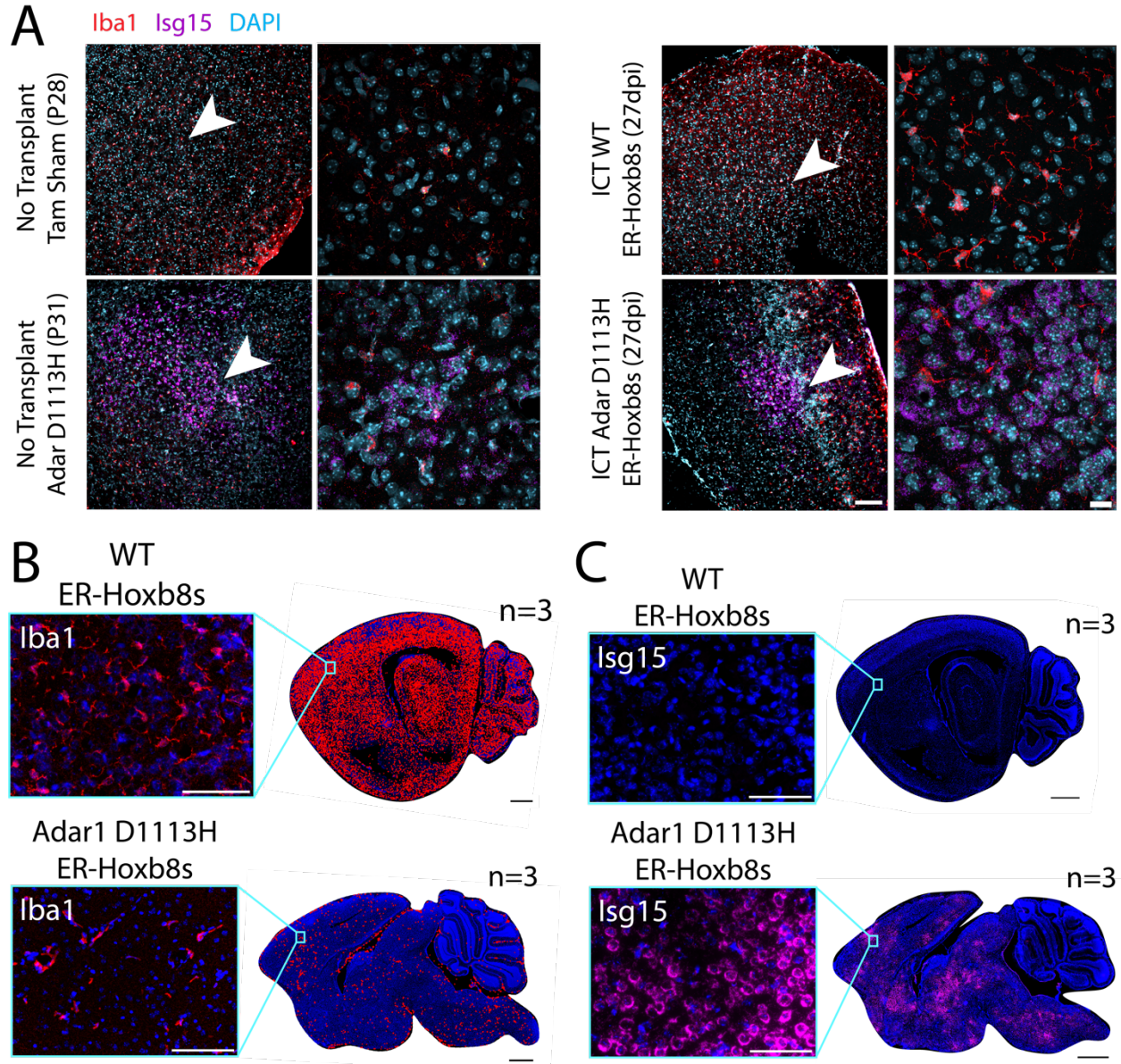
Supplemental Figure 4: Evidence for gene knockout (KO), *Adar1* sgRNA #2 results, and extended bead array data, relating to Figure 4. (A) Heatmap of Log₂ CPM expression of seven causal AGS genes in BMD and ER-Hoxb8 macrophages **(B)** Post-editing trace decomposition charts (via TIDE Analysis) for *Adar1* KO cells targeted with two distinct guides **(C)** ER-Hoxb8 cell counts over time **(D)** Immunostaining of in vitro, eight-day differentiated macrophages comparing control (NTC) and *Adar1* sgRNA #2-transduced macrophages (red = CD11B, blue = DAPI; scale bar = 100um) **(E)** Heatmap showing the Log₂FC (*Adar1* KO values over NTC values) for relevant interferon-stimulated genes for both progenitors and macrophages at baseline **(F)** Validation of in vitro ER-Hoxb8 cell counts with vehicle or 10uM baricitinib treatment using *Adar1* sgRNA #2 **(G)** Interferon, cytokine and chemokine production for ER-Hoxb8 macrophages grown with or without baricitinib, via cytokine bead array **(H)** Trace decomposition charts (via TIDE Analysis) for *Adar1*/*Ifih1* double KO (dKO) cell lines **(I)** Interferon, cytokine and chemokine production for ER-Hoxb8 macrophages with or without subsequent *Ifih1* KO. All p-values calculated via one-way ANOVA with multiple comparisons; ns = not significant or $p \geq 0.05$, * $p < 0.05$, ** $p < 0.01$, *** $p < 0.001$, **** $p < 0.0001$



Supplemental Figure 5: *Adar1* mutation prevents long-term ER-Hoxb8 engraftment in the $Cx3cr1^{CreERT}; Csf1r^{fl/fl}$ mouse, relating to Figure 5. (A) Schematic for in vivo $Cx3cr1^{CreERT}; Csf1r^{fl/fl}$ transplant experiments (B) Representative rendering of donor cell engraftment (scale bar = 1000um) with inset microscopy of GFP+ donor cell engraftment (green = endogenous GFP, blue = DAPI; scale bar = 100um) for control cells (TLR4 KO, NTC) harvested 15 days post-injection, (C) *Adar1* KO cells harvested seven days post-injection, (D) *Adar1/Ifih1* double KO (dKO) cells harvested 13-15 days post-injection, and (E) *Adar1* KO cells harvested three days post-injection



Supplemental Figure 6: Evidence for *Cre* expression, relating to Figure 6. (A) Dual immunostaining/RNA in situ hybridization (ISH) showing IBA1 (red, protein stain), *Cre* (green, ISH), and nuclei (blue, DAPI); scale bar = 100um **(B)** magnified image of a repopulated microglia from the non-transplanted (tam sham control) *Cx3cr1*^{CreERT}; *Csf1r*^{fl/fl} brain shown in (A); scale bar = 10um



Supplemental Figure 7: Extended *Isg15* RNA in situ hybridization (ISH), relating to Figure 6. (A) Corresponding dual immunostaining/RNA ISH depicted by red arrows in Figures 6C/D, showing IBA1 (red, protein stain), *Isg15* (purple, ISH), and nuclei (teal, DAPI); scale bar = 100um; white arrow depicts location of corresponding close up image; scale bar = 20um **(B)** Representative rendering of donor cell engraftment in the *Csf1r^{-/-}* brain (scale bar = 1000um) with inset microscopy of IBA1+ donor cell engraftment (red = IBA1, blue = DAPI; scale bar = 100um) for FVB Osb-GFP WT ER-Hoxb8s and *Adar1* D1113H mutant ER-Hoxb8s harvested 13-14 days post-injection **(C)** Dual immunostaining/RNA ISH for samples shown in (B); tile scale bar = 1000um; inset = *Isg15* (pink, ISH), nuclei (blue, DAPI); scale bar = 100um